Journal of Magnetics 6(2), 73-76 (2001)

Fabrication of Planar Type Inductors Using FeTaN Magnetic Thin Films

Chung-Sik Kim, Seok Bae, Jong-Han Jeong, Seoung-Eui Nam and Hyoung-June Kim

Dept. of Metallurgy and Material Science, Hong-Ik Univ., 72-1 Sangsudong, Mapogu, Seoul 121-791, Korea

(Received 20 September 2000)

A double rectangular spiral type inductor has been fabricated by using FeTaN films. The inductor is composed of internal coils sandwiched by magnetic layers. Characteristics of inductor performance are investigated with an emphasis on planarization of magnetic films. In the absence of the planarizaton process, the grating topology of the upper magnetic films over the coil arrays degrades the soft magnetic properties and the inductor performance. It also induces a longitudinal magnetic anisotropy with the easy axis aligned to the magnetic flux direction. This alignment prevents the upper magnetic films from contributing to the total induction. Glass bonding is a viable method for achieving a completely planar inductor structure. The planar inductor with glass bonding shows excellent performance: inductance of 1.1 μH, Q factor of 7 (at 5 MHz), and the current capability up to 100 mA.

1. Introduction

Planar-type thin film inductors have been increasingly attractive for semiconductor-magnetic integrated circuits because of their high frequency characteristics and compatibility with semiconductor processes [1-3]. To fabricate high performance inductors in a small area, several important factors should be considered, such as magnetic films with good soft magnetism, induction coil with low resistance, and well-designed geometrical inductor structures. Usually, permalloy or Co-based amorphous films have been used for the soft magnetic films. However, in order to improve the inductor performance, especially for high current applications such as DC-DC converters, a soft magnetic material with a higher saturation magnetization ($4\pi M_S$) and high magnetic anisotropy field (Hk) is needed. Many workers have reported that nano-crystalline FeTaN films show high $4\pi M_S$ up to 20 kG as well as excellent soft magnetic characteristics. We used $Fe_{78.8}Ta_{8.5}N_{12.7}$ films for planar type inductors. We also employed a selective electroplating method to fabricate the Cu strip line patterns, which is a suitable method for realizing low resistance Cu coils without pattern etching of Cu lines.

2. Experiment

$Fe_{78.8}Ta_{8.5}N_{12.7}$ films were deposited onto glass substrates (Corning #1737) or Si wafers by DC reactive sputtering. Composition was controlled by varying the area fraction of Ta chips on an Fe target and the partial pressure of N_2 gas. In order to investigate the effects of surface topology on the magnetic properties, $Fe_{78.8}Ta_{8.5}N_{12.7}$ films were first deposited on grating-patterned Si wafer substrates. The depth of the grating was varied from 0~50 μm and the period from 100 μm to 1 mm. The saturation magnetization ($4\pi M_S$) and the coercivity (Hc) of films were measured by B-H loop tracer and vibrating sample magnetometer, and the effective permeability (μ') was measured by the figure-8 coil method and one turn coil method [1].

Double rectangular spiral type inductors, composed of internal Cu coils sandwiched by FeTaN layers, were fabricated. A lower FeTaN film was deposited to a thickness of 2 μm, followed by the sputter-deposition of a 1 μm-thick SiO_2 layer. Cu coils were formed by a selective electroplating method. For seed layers for selective electroplating, 100 Å-thick Cr and 1000 Å-thick Cu layers were consecutively sputter-deposited. After photoresist masking of coil patterns, Cu layers were selective-electroplated to a thickness of 20 μm. The electroplating of Cu was carried out from a $CuSO_4$, H_2SO_4, and $SC(NH_2)_2$ solution at a current density of 60 mA/cm^2. After the photoresist was removed, the Cu and Cr layers were removed using wet etching and ion milling processes, respectively. The seed layers were thin enough that the etching loss of the Cu line during the seed etching was minor.

To fabricate the upper magnetic layer, two different methods were employed. One was to deposit the upper FeTaN layer onto the SiO_2-coated Cu lines without any planarization process. We called this device a "non-planar inductor". In the other method, we deposited a FeTaN film on a separate glass substrate, and subsequently bonded the two glass substrates with surface contact using an epoxy. The latter method provides a completely planar structure, and this device was referred to as a "planar inductor". Samples were

annealed at 400 °C in a vacuum below 5×10^{-5} torr for 0.5 hour to enhance the magnetic properties of FeTaN films as well as to reduce the Cu resistance.

The inductance values were measured by the distributed parameter method using a network analyzer and a micro-strip line with impedance of 50 Ω [5].

3. Results and Discussion

To study the topology effects of FeTaN films, a surface topology with a grating pattern was artificially fabricated on a Si wafer, as schematically shown in Fig. 1. We chose the grating pattern because it resembles the coil configuration of the currently investigated rectangular spiral inductor. Fig. 2 shows the permeability values (μ') at 10 MHz for patterned substrates as a function of grating depths (T_d) at a grating width of 1 mm. For the planar substrate (T_d=0), μ' is high (~2000) in both hard and easy axes, indicating an isotropic magnetic characteristic. The anisotropy field (H_k) of the film is measured to be less than 0.1 Oe.

In the patterned substrates, the magnetic properties are substantially degraded, and the extent of degradation strongly depends on the direction with respect to the grating axis. μ' along the direction parallel to the grating axis decreases more rapidly than that along the perpendicular direction. Reduction of μ' also depends on the grating width (G_w), as shown in Fig. 3. Here, the grating spacing (G_s) and the depth (T_d) are fixed at 100 μm and 20 μm, respectively. The μ' value is substantially low compared to that of the planar topology. Along the parallel direction, the

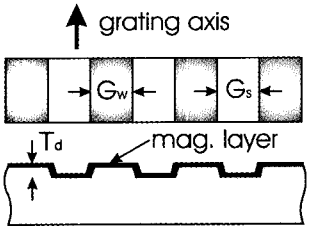

Fig. 1. Schematic diagram of grating pattern on Si wafer.

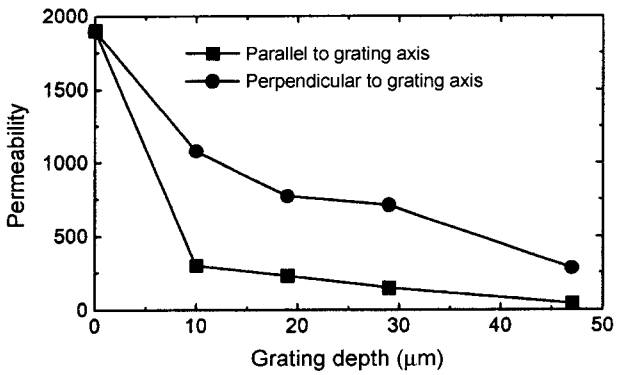

Fig. 2. Permeability (μ) at 10 MHz for patterned substrates as a function of grating depths (T_d). Grating space/width is fixed at 100 mm/1 mm.

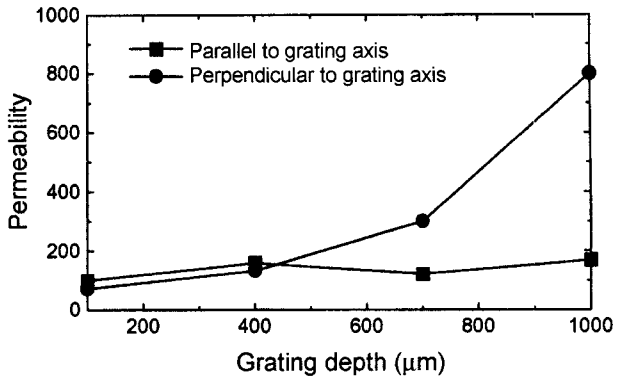

Fig. 3. Permeability (μ') at 10 MHz for patterned substrates as a function of grating width (G_w). Grating space and depth are fixed at 100 μm and 20 μm, respectively.

decreasing width gradually lowers the μ' to reach a minimum value of ~100. Along the perpendicular direction, μ' shows a constant value of ~100, probably already at the minimum value in the investigated width ranges.

To further investigate the topology-induced anisotropy, we observed a Bitter pattern as shown in Fig. 4. The closure domain structure can be clearly observed at the edge of the grating top surface. This domain structure is similar to that typically observed in patterned narrow strips [6]. Since the nucleation of closure domains at the edge of strips comes from the demagnetization field, it is likely that the films are magnetically isolated between the top and the bottom surfaces (or trench wall). This analysis is supplemented by the fact that the permeability dependency on the grating width in Fig. 3 is very similar to that observed in strip patterns [7]. Therefore, analogous explanations for the reduction of permeability in narrow strips can be applied here. That is, the formation of closure domains reduces the high frequency permeability by lowering the spin rotation magnetization, and reduction becomes larger as width decreases.

The structure of the fabricated double rectangular inductor is shown in Fig. 5. The inductor has 10 coil turns, and external dimensions of 7 mm × 10 mm. The width and spacing of Cu coils are fixed at 100 μm. Four different types of inductor structures were fabricated and compared; an air-core inductor (type A), an inductor with a lower magnetic layer only (type B), a non-planar inductor sandwiched

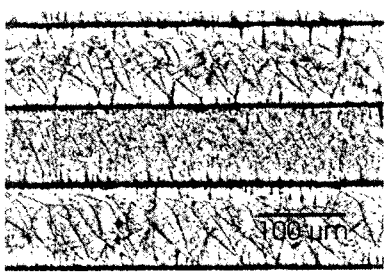

Fig. 4. Bitter pattern for grating sample with T_w and T_S: 100 μm and T_d: 20 μm.

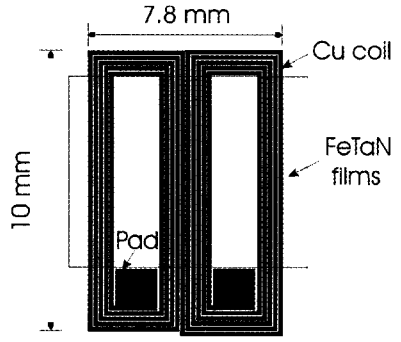

Fig. 5. Structure of the fabricated double rectangular inductor.

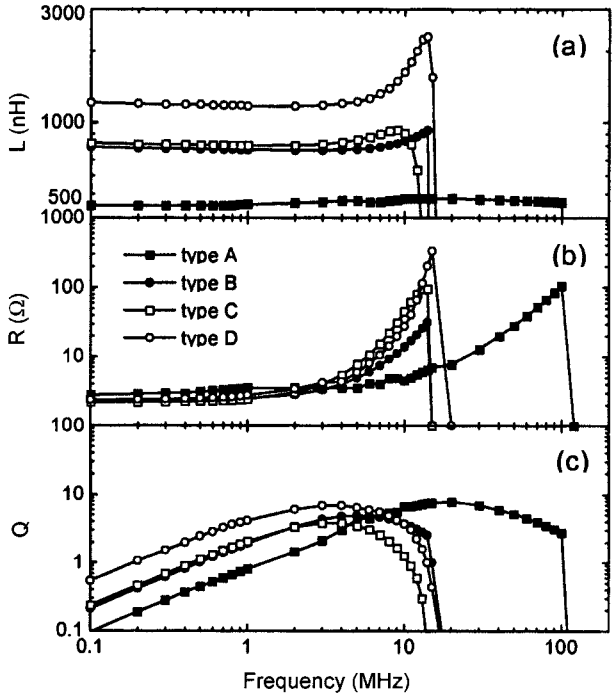

Fig. 6. Characteristics of inductors plotted versus frequency. (a) inductance, (b) resistance, and (c) quality factor.

by two magnetic layers (type C), and a planar inductor sandwiched by two magnetic layers (type D).

Measured inductance values are shown in Fig. 6 as a function of frequency. The air-core inductor shows an inductance value of approximately 460 nH at 1 MHz. The type B inductor shows 780 nH, which is 1.7 times higher than that of the air-core inductor. This value approaches the maximum value of two which has been theoretically predicted by Roshen using the current image method [8]. The type C inductor, the non-planar sandwich inductor, shows an inductance value of 830 nH, indicating a minor enhancement of inductance compared with the half-magnetic-layer inductor. The type D inductor, the planar sandwich inductor, shows a higher inductance value of 1.1 μH.

The negligible enhancement of the type C inductor can be explained in terms of the topology effects, as mentioned earlier. In the type C inductor, the upper magnetic films have the grating topology with a depth of 20 μm (equal to coil thickness) and a width of 100 μm (equal to coil width). From Fig. 3, this topology reduces the permeability to a value less than 100. Thus, the upper magnetic layer makes no significant contribution to the amplitude of magnetic flux. Several workers have proposed closed magnetic circuit structures similar to type C to maximize the magnetic flux conduction [4, 9]. However, the topology effects can diminish the potential advantages of those structures.

As shown in Fig. 6(b), the coil resistance is initially 2 Ω and increases above 1 MHz in the case of magnetic inductors, probably due to proximity effect. The highest quality factor of 7 at 5 MHz is obtained in the type D planar inductor as shown in Fig. 6(c). Even though the value of the Q factor is acceptably high in the DC-DC converter application, further improvement will be possible by reducing the Cu coil resistance by increasing the coil thickness.

High dc current capability of inductors is important for DC-DC converter applications. We measured the inductance value with a superimposed dc current. Fig. 7 shows the results at various frequencies. At all frequencies, the inductance goes down gradually above 100 mA to saturate to a value around 0.6 μH. The fall of inductance above 100 mA is nearly the same as Sato's report for use of CoZrNb films. The current capability of magnetic films is known to be increased with anisotropy field (H_k) as well as with $4\pi M_s$. However, the use of FeTaN, which has a higher $4\pi M_s$ value (17 kG) than CoZrNb (10 kG), apparently does not improve the current characteristic. This may result from the small H_k value of FeTaN. As mentioned earlier, FeTaN films deposited on a planar substrate show a strong magnetic isotropy with a small H_k (~1 Oe), which is much smaller that that of Sato's magnetic-field-annealed CoZrNb film (5.9 Oe). This low H_k value may offset the potential improvement of an increased $4\pi M_s$. In the previous paper, we have reported that a Ti underlayer with field annealing can greatly enhance the anisotropy up to 10 Oe [10]. Employment of this method as a means of improving the current capability is under investigation.

Fig. 8 shows the characteristics of the main circuit efficiency as a function of load current of the buck type con-

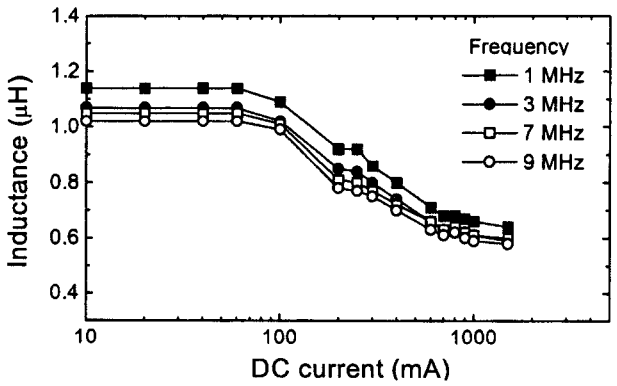

Fig. 7. Inductance value plotted against superimposed dc current at various frequencies.

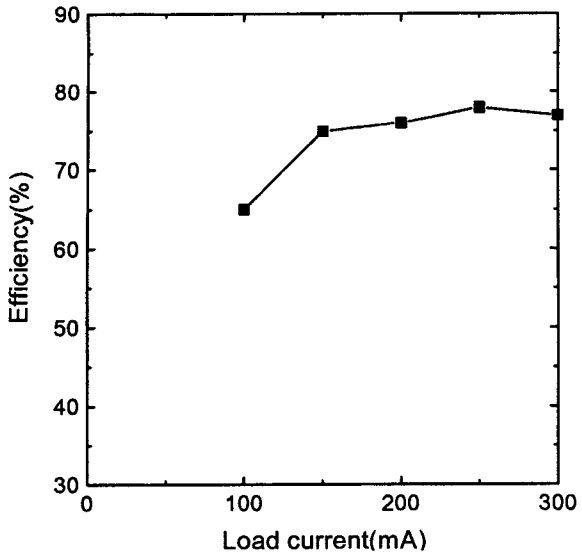

Fig. 8. DC-DC converter efficiency plotted against load current.

verter. Generally, buck type converter that exhibited output voltage is lower than input voltage is kinds of dc-dc converter. Using of planar type inductor loading is wire bonding method for buck type converter. In the buck type converter, the efficiency of inductor is measured of the load current range of 100~300 mA. Efficiency is high in the small load current, then it is advantageous to standby for the cellular phone.

Acknowledgement

The authors gratefully acknowledge the support of the Korean Science and Engineering Foundation under Grant No. N.973010201.

References

[1] T. Kimura et al., J. Magn. Soc. Jpn, **17**, 219 (1993).
[2] R. F. Soohoo, IEEE Trans. Magn., **MAG-15**, 1803 (1979).
[3] K. Kawabe, H. Koyama, and K. Shirae, IEEE Trans. Magn., **MAG-20**, 1805 (1984).
[4] J. Y. Park and M. G. Allen, ISHM '96 Proceedings, 120 (1996).
[5] I. Arai, M. Yamaguchi, and H. Ohzeki, IEEE Trans. Magn., **28**(5), 2175 (1992).
[6] J. S. Y. Feng, and D. A. Thomson, IEEE Trans. Magn., **13**(5), 1521 (1977).
[7] B. C. Webb, M. E. Re, C. V. Jahnes, and M. A. Russak, J. Appl. Phys., **69**(8), 5611 (1991).
[8] W. A. Roshen, Analysis of planar sandwich inductors by current images, IEEE Trans. Magn., **26**(5), 2880 (1990).
[9] M. Yamaguchi, S. Arakawa, H. Ohzeki, Y. Hayashi, and K. I. Arai, IEEE Trans. Magn., **28**(5), 3015 (1992).
[10] D. H. Shin, C. S. Kim, D. H. Ahn, S. E. Nam, and H. J. Kim, J. Appl. Phys., **85**(8), (1999).